Direct detection of spin-orbit effective fields through magneto-optical Kerr effect

T. Xing,[1,2] C. Zhou,[3] C. X. Wang,[1] Z. Li,[1,2] A. N. Cao,[1] W. L. Cai,[1] X. Y. Zhang,[1,2,4] B. Ji,[1] T. Lin,[1] Y. Z. Wu,[3] N. Lei,[1,2,*] Y. G. Zhang,[1] and W. S. Zhao[1,2,†]

[1]*Fert Beijing Institute, BDBC, School of Microelectronics, Beihang University, Beijing 100191, China*

[2]*Beihang-Georgtek Joint Microelectronics Institute, Qingdao Research Institute, Beihang University, Qingdao 266101, China*

[3]*Department of Physics and State Key Laboratory of Surface Physics, Fudan University, Shanghai 200433, China*

[4]*Truth Instrument Co., Ltd., Qingdao 266000, China*

(Received 27 February 2020; revised manuscript received 8 April 2020; accepted 8 April 2020; published 4 June 2020)

Current-induced effective magnetic fields provide efficient methods to electrically control the magnetization switching in ultrathin magnetic films. It is getting clearer that the two terms of spin-orbit torque (SOT), i.e., the dampinglike SOT and the fieldlike SOT, play different roles during the magnetization switching process. Fast and direct estimation of both effective fields are crucial for highly efficient magnetization switching. Methods to extract the amplitudes of the effective fields have been intensively investigated, but they are either complex or require multiparameter fitting, especially for the fieldlike field. We introduce the direct detection of SOT effective fields using hysteresis-loop shift through the magneto-optical Kerr effect in the out-of-plane Pt/Co/W and in-plane Pt/Fe/MgO trilayer systems. The results show strong agreement with transport measurements. Benefiting from noncontact optical detection, our approach in the detection of the spin-orbit effective field has great advantages in the simplified device fabrication processing, and it is suitable not only for metallic systems but also for insulating systems, which paves the way to direct detection of SOT effective fields.

DOI: 10.1103/PhysRevB.101.224407

I. INTRODUCTION

Current-induced spin-orbit torque (SOT) has received a great deal of attention for efficient magnetization manipulation in magnetic memory and logic [1–9]. The SOT has been demonstrated to drive fast domain-wall motion with high efficiency and potentially low power consumption [2,10–14]. It contains two main contributions for spin accumulation, namely the spin-Hall effect (SHE) in heavy metal (HM) and the Rashba effect (RE) induced by broken interfacial symmetry. The SOT comprises two terms, referred to as dampinglike (DL) torque and fieldlike (FL) torque. Recent theory suggests that the FL torque plays a significant role instead of being ignored in SOT switching dynamics [11,15–18]. The experimental work by Baumgartner *et al.* shows that the FL term can promote faster domain wall propagation [19]. The FL torque also favors edge nucleation under the dependence of DMI, external field and the dampinglike torque. The optimization of FL and DL fields in the designed heterostructures is crucial for highly efficient SOT driven magnetization switching. Since the dampinglike torque is mainly from bulk SHE in the thicker HM regime [9], it is possible to estimate the effective field by material selection, while the FL term has a high probability of being related to the HM/ferromagnetic (FM) interface. For different interface processing methods, the fieldlike effective field shows great uncertainty [20,21]. A quick knowledge of the FL term is useful for assessing the efficiency of SOT devices in a timely manner at design stage.

Common methods for quantifying the effective field in perpendicular magnetic anisotropy (PMA) films include anomalous Hall resistance [22], spin-torque FM resonance [1], and SOT-assisted magnetization switching [8], among which the second-harmonic Hall measurement [7,23,24] is the most widely accepted method. For a system with in-plane magnetic anisotropy (IMA), the planar Hall effect (PHE) method is proposed to characterize the combined SOT effective fields in in-plane and out-of-plane orientations. However, those techniques of using parameter fitting to distinguish the DL and FL torques make the measurements and analysis very complex and challenging. They require more intensive data collection and finer data processing. Therefore, those methods may lead to large time consumption in the measurement and lack of accuracy and efficiency.

Experimentally, hysteresis loops are often used as a fast and direct characterization approach. The AHE-based method has been employed to detect the dampinglike torque in the perpendicular direction [4,25–28]. The recent magneto-optical Kerr effect (MOKE) method [21,29–31], while showing its high sensitivity and wide material applicability for SOT, still focuses on dampinglike effective fields. Nevertheless, for the FL effective field, a rapid characterization for PMA and IMA samples is still lacking.

In the present work, we developed and experimented with a fast and direct method by longitudinal MOKE to investigate the FL effective field. We utilized the shift of in-plane hysteresis loops to directly quantify the SOT, which works as a bias for both the PMA and IMA systems. The MOKE method does

*na.lei@buaa.edu.cn

†weisheng.zhao@buaa.edu.cn

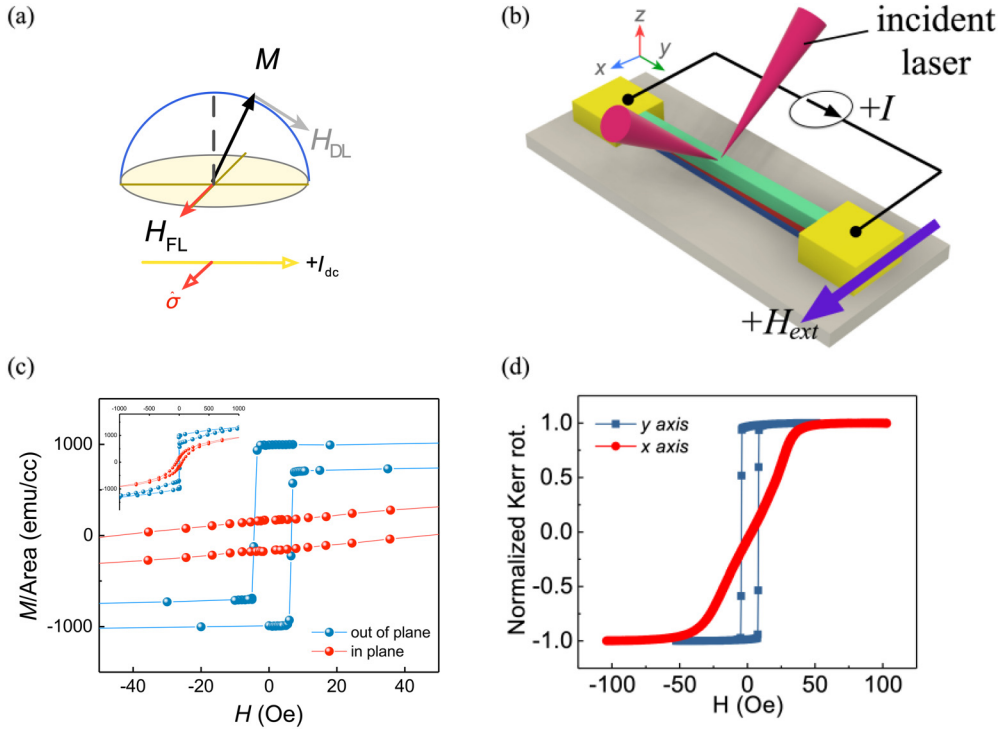

FIG. 1. (a) Schematic representation of the effective fields acting on magnetic moment M_S. H_{FL} is generated by the moment in the $z-y$ plane. (b) Schematic of the longitudinal and polar MOKE measurements for the detection of transverse, longitudinal, and polar effective fields. (c) Out-of-plane and in-plane magnetization of sample (A) vs external magnetic field measured by SQUID. The inset is the same data in the large-field scale. (d) Normalized hysteresis loops measured by MOKE for patterned sample (B) in the longitudinal (y axis) and transverse (x axis) directions.

not require complex device fabrication. Therefore, we could easily obtain the field-like term H_{FL} in the current transverse direction, which is shown in Fig. 1(a).

II. METHOD AND SAMPLE PREPARATION

Figure 1(b) schematically shows that 45° laser incident angle was used to measure the fieldlike term H_{FL} in the longitudinal direction of the stripe-shaped magnetic multilayers. Direct current (dc) ($+I_{dc}$) was applied along the wire ($+y$ axis). Meanwhile, a sweeping magnetic field H_{ex} was applied in the direction of the $+x$. The hysteresis loops were measured using the Durham Magneto Optics NanoMOKE3® with a solid-state laser diode (660 nm, 5 mW). The focused beam spot was 20 nm in the longitudinal geometry, which was smaller than the wire width. We utilized a photodiode bridge to improve the measurement sensitivity up to 0.01 mdeg, and further we used an S-polarized laser to minimize the influence of the MOKE transverse signal.

In terms of experimental verification, first we used sample (A), namely the Ta (2.1)/Pt (5)/Co (0.64)/W (1) system with PMA, to study the in-plane SOT effective field (the numbers in parentheses are the thickness in nanometers). We employed the second-harmonic Hall method for comparison to verify the accuracy of our measurements. Second, IMA sample (B) of Pt (5)/Fe (t_{FM} 0–1)/MgO (5) with a wedged Fe layer was prepared to study the thickness dependence of H_{FL} over the current density. To confirm the magnetic anisotropy, we used a superconducting quantum interference device (SQUID) for sample (A) and a longitudinal MOKE measurement for sample (B), which are shown in Figs. 1(c) and 1(d) [32]. All films were patterned into 100-μm-wide channels [a Hall bar structure for sample (A) and a wire along the Fe wedge for sample (B)] by photolithography and the Ar^+ ion-milling process. All measurements were performed at room temperature (the second-harmonic Hall measurement contained the temperature control).

According to the fieldlike torque $\tilde{\tau}_{FL} = -H_{FL}M_S(\hat{m} \times \hat{\sigma})$, where $\hat{m}$ is the unit vector of saturation magnetization of the layer (M_S) [21,33], the direction of the effective field can be determined by the polarization of the electron spins ($\hat{\sigma}$), which is expressed by $\tilde{H}_{FL} = H_{FL}\hat{\sigma}$ [34–36]. By compensating for the SOT-induced broken symmetry of the switching fields, an effective field H_{eff} could be obtained using the horizontal shift of the switching field of up-to-down (down-to-up) reversal [26]. The offset field is expressed as $H_{offset}(I) = -H_{eff}(I) + H(I^2) + H_0$, where $H(I^2)$ represents the symmetric term of the current polarity due to Joule heating, and H_0 represents the current-independent term from the residual field and the quadratic MOKE [34]. The SOT effective field could be extracted by subtracting the positive and negative current values, written as $H_{SOT} = [H_{offset}(+I) - H_{offset}(-I)]/2$ based on its odd symmetry. For the fieldlike measurement, the Oersted field should be considered. Because of the shutting effect, the Oersted field in the FM layer could be estimated as follows: $H_{Oersted} = -J_{HM}t_{HM}/2$, where t_{HM} is the HM thickness. Therefore, the effective field of H_{FL} is expressed as follows: $H_{FL} = [H_{offset}(+I) - H_{offset}(-I)]/2 - H_{Oersted}$.

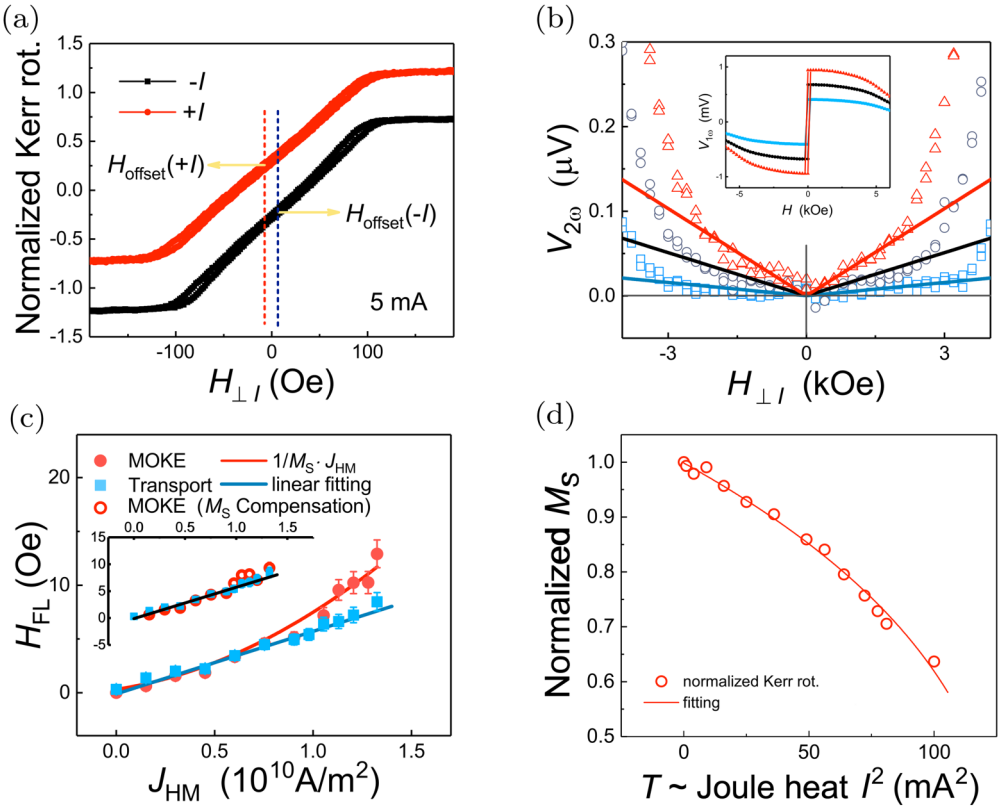

FIG. 2. (a) Normalized hysteresis loops of sample (A) (Pt/Co/W) for the fieldlike field measurement under dc currents of ±5 mA. For clarity, appropriate vertical offsets were added. (b) First- (1ω) and second- (2ω)harmonic voltage in the transverse configuration. (c) Comparisons of the MOKE (red dots) and transport measurements (blue squares) for the fieldlike term. The linear fitting of the transport results is shown by the solid blue line. The MOKE results are fitted with $(1/M_S)J_{HM}$ shown by the solid red line. Inset: the MOKE results corrected by M_S show a good linear fit by the solid blue line from the transport method. (d) Normalized M_S decays with Joule heat I^2, which is proportional to temperature T.

III. RESULTS AND DISCUSSION

A. Measurement in the PMA system

The large spin-orbit coupling system of Pt/Co/W was selected for demonstration. The magnetic moment in Pt/Co/W wire was first magnetized along the $+z$ direction. The longitudinal MOKE with a magnetic field applied along the x direction is performed to measure the FL fields induced by currents. Figure 2(a) shows the typical normalized hysteresis loops for the H_{FL} measurements with $I_{dc} = \pm 5$ mA. We can see that the horizontal shift corresponds to the sign of the current polarity, which indicates that in-plane effective fields were clearly observed.

For comparison, the first- and second-harmonic Hall voltages were detected at 3, 5, and 7 mA alternating current with a frequency ω of 133 Hz, as shown in Fig. 2(b). Note that for extracting the SOT effective fields precisely, both contributions of the AHE and the planar Hall effect (PHE) were considered [23,32]. Figure 2(c) shows a summary of the numerical comparisons between MOKE and the second-harmonic Hall methods for the fieldlike field, respectively. At low current densities, the MOKE and second-harmonic Hall methods displayed a high level of equivalence, while at a high current density (above 1×10^{10} A/m^2) an exponential increase could be seen in the MOKE method, leading to failure in the linear fitting. According to the expression of the SOT-induced effective field,

$$H_{SOT} = \frac{\hbar}{2e}\frac{\xi_{SH}}{M_S t_{FM}} J_{HM}, \tag{1}$$

where $\hbar$ is the reduced Planck constant, e is the elemental charge of an electron, t_{FM} is the thickness of the magnetic layer, and ξ_{SH} is the spin-Hall efficiency. The linear fitting is based on the assumption that M_S is constant. Note that the Curie temperature of the FM layer decreases dramatically with a decrease in the film thickness in the ultrathin regime. Thus, the temperature increase from current-induced Joule heating presumably approaches the Curie temperature of 0.6 nm Co in our film. In our transport setup, a well-controlled temperature feedback system ensures a stable temperature and constant M_S under applied currents [32]. Therefore, a good linear fitting is shown by the solid blue line in Fig. 2(c). However, M_S decreases with an increase in the amplitude of applied currents in the MOKE method due to the lack of temperature control, which is shown in Fig. 2(d). Since the Joule heating represented by I^2 is proportionally converted to temperature, the change in M_S can be well described using the fitting of $M_S \sim (T_C - T)^{1/3}$ (the estimated T_C is 610 K) [32]. This result is consistent with the previous study on SOT efficiency at different temperatures [37]. Taking the M_S variation with the current density (please see the supplementary note 3 in Ref. [32]), the FL fields from the MOKE method

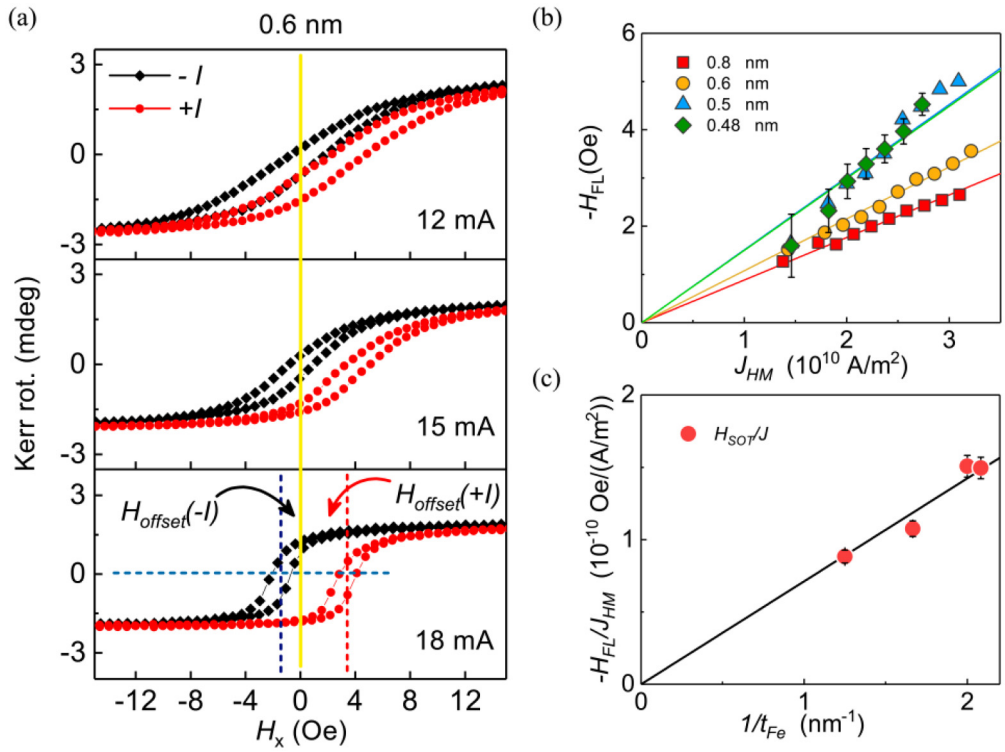

FIG. 3. (a) Hysteresis loops measured by the longitudinal MOKE for sample (B) [Pt (5)/Fe ($t_{FM} = 0.6$ nm)/MgO (5)] under dc current of $\pm I$. H_{offset} ($H_{eff} = -H_{offset}$) represents the effective field due to SOT. (b) SOT effective field (H_{FL}) at different thicknesses as a function of the current density. (c) H_{DL}/J_{HM} as a function of $1/t_{FM}$. The solid lines show linear fitting of the data.

show an obvious agreement with those from the transport method shown in the inset of Fig. 2(c). From the linear fitting, the slope of H_{FL} versus J_{HM} was observed to be 5.8 Oe per 1×10^{10} A/m^2.

B. Measurement in the IMA system

For sample (B) with $t_{FM} = 0.6$ nm, loops at several typical currents are shown in Fig. 3(a) to characterize H_{eff} as a function of the applied dc current. For different current amplitudes and polarities, the shifts in the hysteresis loops increased with the current density and separated in the opposite direction, meaning that the effective field was current-dependent. Under current $I = +18$ mA, the center of the hysteresis loop shifted to the positive side, presenting a negative effective field. Meanwhile, the Oersted field according to Ampere's law had an opposite sign, which indicates that a fieldlike torque in the system existed. Because Pt is known to have a positive spin-Hall angle, H_{FL} should have the same direction as the Oersted field. However, the measured direction of H_{FL} was opposite that of the contribution of SHE, which means that RE must overcome these two contributions and dominated in the system. This result is also consistent with the reported data measured by PHE [38,39].

We then investigated the thickness dependence of the FM layer by focusing the laser spots at several different positions of the thickness wedge sample. Figure 3(b) shows our H_{FL} summary at different thicknesses as a function of the current density. The current density in the HM layer was calculated from the multi-layer shunt model. Figure 3(c) shows the slope of H_{FL}/J_{HM} versus thickness of the FM layer ($1/t_{FM}$), which were found to have a good linear relationship as expected from Eq. (1). The Oersted field was calculated to be ~0.3 Oe per 1×10^{10} A/m^2. As the thickness decreased, the ratio of the fieldlike term to the current density increased from 0.9×10^{-10} to 1.6×10^{-10} Oe/(A/m^2), reaching a maximum at 0.48 nm. The dependence of the fieldlike SOT fields on the thickness of Fe conformed to the result obtained by Kawaguchi [39]. We note that the Pt/Fe system had a strong quadratic MOKE [40], which made H_C quite sensitive to the angle between the crystal orientation and the measurement direction. However, the effective field signal came from the offset of symmetry, as previously analyzed. The change in H_C would not affect the detection accuracy.

C. Calculation of spin-Hall efficiency

For comparison, total spin-Hall efficiency ξ_{SH} [20] was calculated. The calculation method of spin efficiency can be directly derived from the detected values and be rewritten as follows:

$$\xi_{SH} = \frac{2eM_S t_{FM}}{\hbar}\frac{H_{FL}}{J_{HM}}.$$

In addition, introducing decreasing M_S into the equation could eliminate the current-induced thermal effects on the calculation. Here, with the increase in J_{HM}, M_S decreased from 1000 to 830 emu/cm^3 and $t_{FM} = 0.64$ nm. The fieldlike spin-Hall efficiency was calculated to be 0.12 ± 0.02. We also compare the results measured by the harmonic Hall technique.

ξ_{SH} was calculated to be 0.34 (dampinglike term) and 0.12 (fieldlike term), respectively, showing that the error between these two techniques is less than 10%.

IV. CONCLUSION

In summary, we have demonstrated a direct method to detect FL effective fields for both PMA and IMA systems. Compared with the transport method, our method shows good consistency and flexibility. Simultaneously, the change in M_S affected by the current-induced Joule heating can be used to describe the nonlinear behavior of effective fields versus current density, indicating that the arrangement of the magnetic moment engineering may play a role in the SOT manipulation. The measurement we presented provides a direct and convenient method to quantify SOT effective fields.

ACKNOWLEDGMENTS

This work was supported by the National Natural Science Foundation of China (Grants No. 11574018, No. 11974079, No. 11734006, and No. 61627813), by International Collaboration Project B16001, by the ed by the National Key Technology Program of China (No. 2017ZX01032101), and by the Program of Shanghai Academic Research Leader (No. 17XD1400400). All authors would like to thank Albert Fert for the fruitful discussion.

[1] L. Liu, T. Moriyama, D. C. Ralph, and R. A. Buhrman, Phys. Rev. Lett. **106**, 036601 (2011).
[2] L. Liu, C.-F. Pai, Y. Li, H. Tseng, D. Ralph, and R. Buhrman, Science **336**, 555 (2012).
[3] K. Ando, S. Takahashi, K. Harii, K. Sasage, J. Ieda, S. Maekawa, and E. Saitoh, Phys. Rev. Lett. **101**, 036601 (2008).
[4] G. Yu, P. Upadhyaya, Y. Fan, J. G. Alzate, W. Jiang, K. L. Wong, S. Takei, S. A. Bender, L.-T. Chang, Y. Jiang, M. Lang, J. Tang, Y. Wang, Y. Tserkovnyak, P. K. Amiri, and K. L. Wang, Nat. Nanotechnol. **9**, 548 (2014).
[5] I. M. Miron, K. Garello, G. Gaudin, P.-J. Zermatten, M. V. Costache, S. Auffret, S. Bandiera, B. Rodmacq, A. Schuhl, and P. Gambardella, Nature (London) **476**, 189 (2011).
[6] I. M. Miron, G. Gaudin, S. Auffret, B. Rodmacq, A. Schuhl, S. Pizzini, J. Vogel, and P. Gambardella, Nat. Mater. **9**, 230 (2010).
[7] J. Kim, J. Sinha, M. Hayashi, M. Yamanouchi, S. Fukami, T. Suzuki, S. Mitani, and H. Ohno, Nat. Mater. **12**, 240 (2013).
[8] L. Liu, O. J. Lee, T. J. Gudmundsen, D. C. Ralph, and R. A. Buhrman, Phys. Rev. Lett. **109**, 096602 (2012).
[9] R. Ramaswamy, J. M. Lee, K. Cai, and H. Yang, Appl. Phys. Rev. **5**, 031107 (2018).
[10] A. V. Khvalkovskiy, V. Cros, D. Apalkov, V. Nikitin, M. Krounbi, K. A. Zvezdin, A. Anane, J. Grollier, and A. Fert, Phys. Rev. B **87**, 020402(R) (2013).
[11] S. Fukami, T. Anekawa, C. Zhang, and H. Ohno, Nat. Nanotechnol. **11**, 621 (2016).
[12] X. Zhao, X. Zhang, H. Yang, W. Cai, Y. Zhao, Z. Wang, and W. Zhao, Nanotechnology **30**, 335707 (2019).
[13] X. Zhang, N. Vernier, L. Vila, S. Yan, Z. Cao, A. Cao, Z. Wang, W. Cai, Y. Liu, H. Yang, D. Ravelosona, and W. Zhao, Phys. Rev. Appl. **11**, 054041 (2019).
[14] L. Zhang, X. Zhang, M. Wang, Z. Wang, W. Cai, K. Cao, D. Zhu, H. Yang, and W. Zhao, Appl. Phys. Lett. **112**, 142410 (2018).
[15] T. Taniguchi, S. Mitani, and M. Hayashi, Phys. Rev. B **92**, 024428 (2015).
[16] W. Legrand, R. Ramaswamy, R. Mishra, and H. Yang, Phys. Rev. Appl. **3**, 064012 (2015).
[17] J. Park, G. E. Rowlands, O. J. Lee, D. C. Ralph, and R. A. Buhrman, Appl. Phys. Lett. **105**, 102404 (2014).
[18] M. Wang, W. Cai, D. Zhu, Z. Wang, J. Kan, Z. Zhao, K. Cao, Z. Wang, Y. Zhang, T. Zhang, C. Park, J.-P. Wang, A. Fert, and W. Zhao, Nat. Electron. **1**, 582 (2018).
[19] M. Baumgartner, K. Garello, J. Mendil, C. O. Avci, E. Grimaldi, C. Murer, J. Feng, M. Gabureac, C. Stamm, Y. Acremann, S. Finizio, S. Wintz, J. Raabe, and P. Gambardella, Nat. Nanotechnol. **12**, 980 (2017).
[20] C.-F. Pai, Y. Ou, L. H. Vilela-Leão, D. C. Ralph, and R. A. Buhrman, Phys. Rev. B **92**, 064426 (2015).
[21] X. Fan, H. Celik, J. Wu, C. Ni, K.-J. Lee, V. O. Lorenz, and J. Q. Xiao, Nat. Commun. **5**, 3042 (2014).
[22] T. Suzuki, S. Fukami, N. Ishiwata, M. Yamanouchi, S. Ikeda, N. Kasai, and H. Ohno, Appl. Phys. Lett. **98**, 142505 (2011).
[23] M. Hayashi, J. Kim, M. Yamanouchi, and H. Ohno, Phys. Rev. B **89**, 144425 (2014).
[24] M. Akyol, J. G. Alzate, G. Yu, P. Upadhyaya, K. L. Wong, A. Ekicibil, P. K. Amiri, and K. L. Wang, Appl. Phys. Lett. **106**, 032406 (2015).
[25] J. Finley and L. Liu, Phys. Rev. Appl. **6**, 054001 (2016).
[26] C.-F. Pai, M. Mann, A. J. Tan, and G. S. D. Beach, Phys. Rev. B **93**, 144409 (2016).
[27] J. Han, A. Richardella, S. A. Siddiqui, J. Finley, N. Samarth, and L. Liu, Phys. Rev. Lett. **119**, 077702 (2017).
[28] G. Yu, L.-T. Chang, M. Akyol, P. Upadhyaya, C. He, X. Li, K. L. Wong, P. K. Amiri, and K. L. Wang, Appl. Phys. Lett. **105**, 102411 (2014).
[29] T.-Y. Tsai, T.-Y. Chen, C.-T. Wu, H.-I. Chan, and C.-F. Pai, Sci. Rep. **8**, 5613 (2018).
[30] Y. Chen, H. Celik, T. Wang, H. Kannan, I. N. Krivorotov, and J. Q. Xiao, Phys. Rev. B **95**, 144405 (2017).
[31] M. Montazeri, P. Upadhyaya, M. C. Onbasli, G. Yu, K. L. Wong, M. Lang, Y. Fan, X. Li, P. K. Amiri, R. N. Schwartz, C. A. Ross, and K. L. Wang, Nat. Commun. **6**, 8958 (2015).
[32] See Supplemental Material at http://link.aps.org/supplemental/10.1103/PhysRevB.101.224407 for details of the sample preparation, which include Ref. [41]; for details of the second-harmonic measurement, planar Hall effect contribution, and temperature control, which include Refs. [23,30,42]; and for details on the fitting of Curie temperature and the decrease of saturation magnetization with Joule heating (temperature), which include Ref. [43].
[33] A. Manchon and S. Zhang, Phys. Rev. B **78**, 212405 (2008).
[34] X. Fan, J. Wu, Y. Chen, M. J. Jerry, H. Zhang, and J. Q. Xiao, Nat. Commun. **4**, 1799 (2013).
[35] F. Luo, S. Goolaup, W. C. Law, S. Li, F. Tan, C. Engel, T. Zhou, and W. S. Lew, Phys. Rev. B **95**, 174415 (2017).

[36] P. M. Haney, H.-W. Lee, K.-J. Lee, A. Manchon, and M. D. Stiles, Phys. Rev. B **87**, 174411 (2013).
[37] W. Seung Ham, S. Kim, D.-H. Kim, K.-J. Kim, T. Okuno, H. Yoshikawa, A. Tsukamoto, T. Moriyama, and T. Ono, Appl. Phys. Lett. **110**, 242405 (2017).
[38] M. Kawaguchi, K. Shimamura, S. Fukami, F. Matsukura, H. Ohno, T. Moriyama, D. Chiba, and T. Ono, Appl. Phys. Express **6**, 113002 (2013).
[39] M. Kawaguchi, T. Moriyama, T. Koyama, D. Chiba, and T. Ono, J. Appl. Phys. **117**, 17C730 (2015).
[40] M.-L. Zhang, Y. Jun, L. Rui, M. Shu, X. Yong, L. Hao-Liang, H. Chris Van, and C. Zi-Yu, Chin. Phys. B **25**, 047503 (2016).
[41] J. X. Li, M. W. Jia, Z. Ding, J. H. Liang, Y. M. Luo, and Y. Z. Wu, Phys. Rev. B **90**, 214415 (2014).
[42] J. W. Lee, Y.-W. Oh, S.-Y. Park, A. I. Figueroa, G. van der Laan, G. Go, K.-J. Lee, and B.-G. Park, Phys. Rev. B **96**, 064405 (2017).
[43] Y. Quessab, R. Medapalli, M. S. El Hadri, M. Hehn, G. Malinowski, E. E. Fullerton, and S. Mangin, Phys. Rev. B **97**, 054419 (2018).